JOURNAL OF PHYSICAL ORGANIC CHEMISTRY, VOL. 10, 254–272 (1997)

REVIEW COMMENTARY
π–π INTERACTIONS IN SELF-ASSEMBLY

CHRISTIAN G. CLAESSENS AND J. FRASER STODDART*
School of Chemistry, University of Birmingham, Edgbaston, Birmingham B15 2TT, UK

The recent surge of interest in the control of molecular organization in both the solution state (i.e. self-assembly) and the solid state (i.e. crystal engineering) has led researchers to recognize increasingly the importance of weak non-covalent interactions. The design and synthesis of an efficient molecular construction set are dependent upon a very close interplay between x-ray crystallography and synthetic chemistry. π–π Stacking interactions between π-donors, such as hydroquinone, resorcinol or dioxynaphthalene residues, and π-accepting ring systems, such as bipyridinium or π-extended viologen units, can govern the self-assembly of a variety of complexes and interlocked molecular compounds in both the solid and solution states. Non-covalent bonding interactions (i.e. π–π interactions) can be considered as information vectors: they define and rule the self-assembly processes that lead to the formation of the desired molecular and supramolecular architectures, and thereafter they still govern the dynamic processes occurring within the self-assembled structures and superstructures. The manner in which such molecules and supermolecules can contribute to an understanding of non-covalent interactions at both structural and superstructural levels is described, with reference to numerous examples of self-assembly processes in synthesis, of dynamic processes in the solution state, and of the packing of molecules and molecular complexes in the solid state. © 1997 by John Wiley & Sons, Ltd.

J. Phys. Org. Chem. **10**, 254–272 (1997) No. of Figures: 31 No. of Tables: 4 No. of References: 33
Keywords: π–π interactions; self-assembly; catenanes; cyclophanes
Received 11 October; revised November 1996; accepted 21 November 1996

INTRODUCTION

A fundamental understanding of the nature of the non-covalent bond is of utmost importance in the identification of molecules capable of self-assembling in solution and of self-organizing in the solid state. So far, chemists have been able to generate, in both solution and the solid state, through the methodology of self-assembly,[1] a wide variety of synthetic molecular and supramolecular architectures which include double-stranded helicates,[2] liquid crystals,[3] molecular crystals,[4] hydrogen-bonded aggregates,[5] receptor–substrate complexes[6] and Langmuir–Blodgett films.[7] Initially in Sheffield, and subsequently in Birmingham, we have developed a synthetic methodology for the template-directed syntheses of mechanically interlocked molecular compounds, such as catenanes and rotaxanes via precatenanes and pseudorotaxanes. Their self-assembly in solution is driven mainly by π–π interactions[8] and, to a marginally lesser extent, by weak hydrogen bonding and edge-to-face T-type interactions.[9] The driving force for the self-assembly of these systems usually relies on several molecular recognition events that include the π–π stacking interactions which occur between a π-electron-deficient unit, such as a bipyridinium dication, and a π-electron-rich unit, such as a hydroquinone ring; they also include orthogonally directed [CH · · · O] hydrogen bonds and [CH · · · π] interactions. In order to exploit the novel properties already being exhibited by some of these architectures, a more fundamental understanding of the non-covalent interactions that give rise to these properties is required. That is why, by systematically studying small variations in similar systems, we hope to discern precisely the various contributions that are responsible for the formation and/or the organization of the molecular assemblies and supramolecular arrays. We are now in possession of an enormous amount of data regarding these systems, and everyday our still empirically driven approach to their design and synthesis is improving by leaps and bounds.

DISCUSSION

Descriptors

It is convenient at this point to explain the acronyms used in the illustrations that appear in the tables and figures: HQ

* *Correspondence to:* J. F. Stoddart.
Contract grant sponsor: Biotechnology and Biological Sciences Research Council.
Contract grant sponsor: Engineering and Physical Sciences Research Council.

 CCC 0894–3230/97/050254–19 $17.50

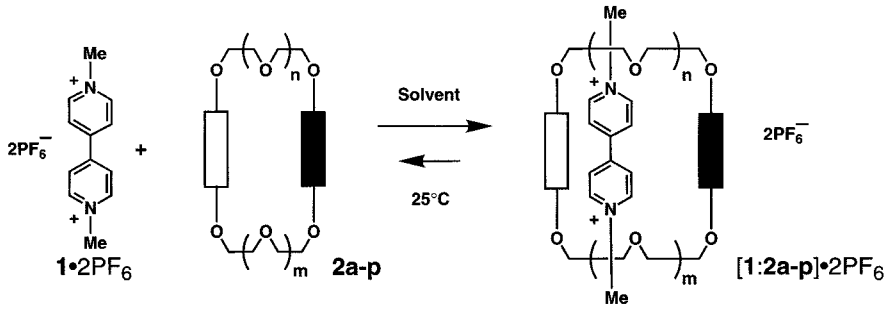

Crown Ether			m	n	Crown Ether			m	n	Crown Ether			m	n
2a	HQ	HQ	2	1	2g	HQ	1/6DN	3	3	2m	1/5DN	1/6DN	3	3
2b	HQ	HQ	2	2	2h	HQ	2/6DN	3	3	2n	1/5DN	2/6DN	3	3
2c	HQ	HQ	3	2	2i	HQ	2/7DN	3	3	2o	1/5DN	2/7DN	3	3
2d	HQ	HQ	3	3	2j	1/5DN	1/5DN	3	3	2p	2/6DN	2/7DN	3	3
2e	HQ	HQ	4	3	2k	1/6DN	1/6DN	3	3					
2f	HQ	HQ	4	4	2l	2/7DN	2/7DN	3	3					

Figure 1. Complexation of paraquat $\mathbf{1}\cdot 2PF_6$ by the π-electron-rich macrocyclic polyethers **2a**–**p**

stands for hydroquinone, Res for resorcinol and X/X-DN for an X,X-disubstituted dioxynaphthalene unit.

Molecular recognition

Macrocyclic polyethers containing two π-electron rich components have been shown[10] to act as suitable receptors for the bypiridinium herbicide paraquat $\mathbf{1}\cdot 2PF_6$ (Figure 1).The basic strategy behind the polyether design relied in the beginning on (i) the potentially favourable π–π interactions between the π-electron-deficient units in paraquat $\mathbf{1}\cdot PF_6$ and the π-electron-rich aromatic ring systems of the crown ether moiety, and (ii) a good stereoelectronic match between the components.

Among the series of crown ethers containing two hydroquinone rings linked by polyether chains of various length (**2a**–**f**, Figure 1), the macrocyclic polyether **2d**, incorporating two tetraethylene glycol linkers, is the one that forms[10a] the strongest 1:1 complex with paraquat $\mathbf{1}\cdot 2PF_6$ in Me_2CO. Quantitative analysis of the complex $[\mathbf{1}:\mathbf{2d}]\cdot 2PF_6$ formed in acetone, by UV spectrophotometry, revealed a charge-transfer band centred on 435 nm. Not only did it provide evidence for the 1:1 stoichiometry of the complex but it also afforded a value of 730 l mol^{-1} for its stability constant (K_a), corresponding to a free energy of complexation ($\Delta G°$) of -3.9 kcal mol^{-1} (1 kcal = 4.184 kJ). The solid-state structure of $[\mathbf{1}:\mathbf{2d}]\cdot 2PF_6$ (Figure 2) revealed a pseudorotaxane-like incorporation of the paraquat unit, sandwiched in between the parallel-aligned hydroquinone rings of the receptor. The distance between the mean plane

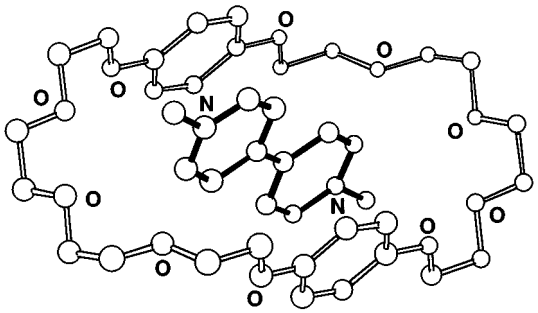

Figure 2. Ball-and-stick representation of the solid-state structure of the complex $[\mathbf{1}:\mathbf{2d}]^{2+}$

Table 1. Free energies of complexation ($-\Delta G°$) for the 1:1 complexes $[\mathbf{1}:\mathbf{2a}–\mathbf{p}]\cdot 2PF_6$ at 25 °C

Complex	$-\Delta G°$ (kcal mol^{-1})	Complex	$-\Delta G°$ (kcal mol^{-1})
$[\mathbf{1}:\mathbf{2a}]\cdot 2PF_6$	0[a]	$[\mathbf{1}:\mathbf{2i}]\cdot 2PF_6$	3.6[b]
$[\mathbf{1}:\mathbf{2b}]\cdot 2PF_6$	1.8[a]	$[\mathbf{1}:\mathbf{2j}]\cdot 2PF_6$	4.2[b]
$[\mathbf{1}:\mathbf{2c}]\cdot 2PF_6$	2.8[a]	$[\mathbf{1}:\mathbf{2k}]\cdot 2PF_6$	3.6[b]
$[\mathbf{1}:\mathbf{2d}]\cdot 2PF_6$	3.9[a]	$[\mathbf{1}:\mathbf{2l}]\cdot 2PF_6$	4.1[b]
$[\mathbf{1}:\mathbf{2e}]\cdot 2PF_6$	3.2[a]	$[\mathbf{1}:\mathbf{2m}]\cdot 2PF_6$	3.6[b]
$[\mathbf{1}:\mathbf{2f}]\cdot 2PF_6$	3.0[a]	$[\mathbf{1}:\mathbf{2n}]\cdot 2PF_6$	4.0[b]
$[\mathbf{1}:\mathbf{2g}]\cdot 2PF_6$	3.2[b]	$[\mathbf{1}:\mathbf{2o}]\cdot 2PF_6$	4.0[b]
$[\mathbf{1}:\mathbf{2h}]\cdot 2PF_6$	3.6[b]	$[\mathbf{1}:\mathbf{2p}]\cdot 2PF_6$	4.0[b]

[a]Determined in Me_2CO.
[b]Determined in MeCN.

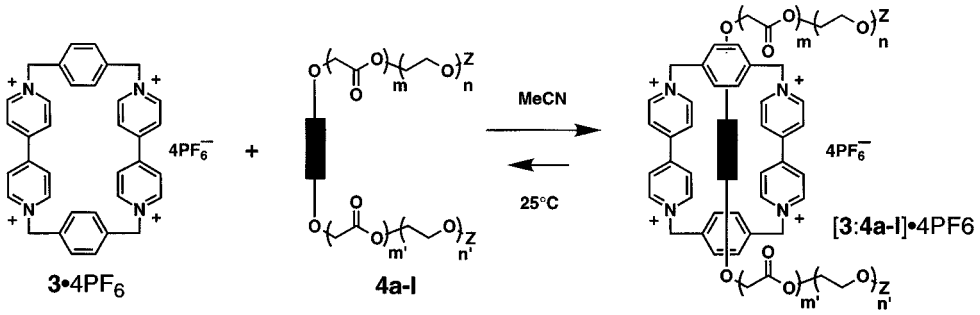

Guest		m	n	m'	n'	Z	Guest		m	n	m'	n'	Z
4a	HQ	0	0	0	0	H	4g	2/6DN	0	2	0	2	H
4b	HQ	0	1	0	1	H	4h	2/7DN	0	2	0	2	H
4c	HQ	0	2	0	2	H	4i	1/5DN	0	2	0	2	H
4d	HQ	0	3	0	3	H	4j	HQ	0	2	0	2	Me
4e	HQ	0	4	0	4	H	4k	HQ	1	1	1	1	Me
4f	1/6DN	0	2	0	2	H	4l	HQ	1	1	1	1	Me

Figure 3. Complexation of the π-electron-rich guests **4a**–**l** by the tetracationic cyclophane **3**·4PF_6

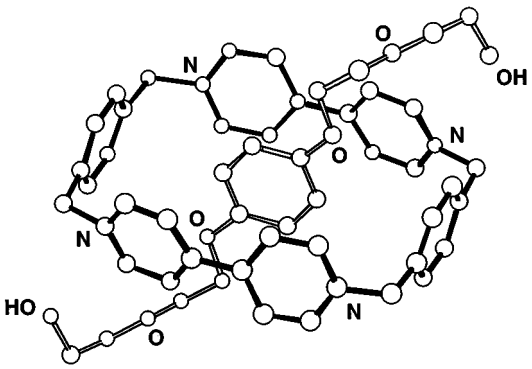

Figure 4. Ball-and-stick representation of the solid-state structure of the complex [**3**·**4c**]$^{4+}$

Table 2. Free energies of complexation ($-\Delta G°$) for the 1:1 complexes [**3**:**4a**–**l**]·4PF_6 at 25 °C in MeCN

Complex	$-\Delta G°$ (kcal mol^{-1})	Complex	$-\Delta G°$ (kcal mol^{-1})
[**3**:**4a**]·4PF_6	1.7	[**3**:**4g**]·4PF_6	3.5
[**3**:**4b**]·4PF_6	3.3	[**3**:**3h**]·4PF_6	3.1
[**3**:**4c**]·4PF_6	4.6	[**3**:**4i**]·4PF_6	5.1
[**3**:**4d**]·4PF_6	4.6	[**3**:**4j**]·4PF_6	4.9
[**3**:**4e**]·4PF_6	4.6	[**3**:**4k**]·4PF_6	3.9
[**3**:**4f**]·4PF_6	3.2	[**3**:**4l**]·4PF_6	3.7

of the paraquat dication and the mean planes of each of the hydroquinone rings is *ca* 3.5 Å and the central axis of the dication ($N^+ \cdots N^+$) is tilted by *ca* 28° with respect to the O · · · O axes of the hydroquinone rings. This excellent complementarity is a consequence of the combination of a good geometric match and favourable non-covalent bonding interactions which are: (i) electrostatic interactions involving the phenolic oxygen atoms, (ii) [C—H · · · O][11] and van der Waals interactions involving the polyether chains and (iii) dispersive and charge-transfer interactions involving the hydroquinone rings and different parts of the paraquat dication.

Another series of crown ethers possessing the same polyether chains as in **2d**, but containing different aromatic (**2g**–**p**, Figure 1) units, has been synthesized and complexation studies with **1**·2PF_6 were carried out in MeCN.[10b,c] It appeared from this study that crown ethers containing 1/5-, 1/6-, 2/6- and 2/7-disubstituted dioxynaphthalene units (**2g**–**p**, Figure 1) also bind paraquat **1**·2PF_6 but with significantly different free energies of complexation $\Delta G°$ (Table 1), showing how subtle changes in the substitution pattern of the dioxynaphthalene units can affect dramatically the molecular recognition process.

The mode of complexation of paraquat by **2d** led us to propose that it might be possible to reverse constitutionally the roles of the receptor and the substrate and so bind a π-electron-rich unit inside a tetracationic molecular receptor. Such a receptor is the tetracation cyclobis(paraquat-*p*-phenylene) **3**$^{4+}$, which incorporates (Figure 3) two π-electron-deficient paraquat residues connected in a

Table 3. Free energies of complexation ($-\Delta G°$) for the 1:1 complexes between **3**·4Cl and various amino acids and neurotransmitters at 25 °C in aqueous solution

Complex	$-\Delta G°$ (kcal mol^{-1})	Complex	$-\Delta G°$ (kcal mol^{-1})
[**3**:tryptophan]·4Cl	3.7–3.9[a]	[**3**:serotonin]·4Cl	4.1[a]
[**3**:tyrosine]·4Cl	3.5–3.7[a]	[**3**:phenyl β-D-glucoside]·4Cl	4.9[c]
[**3**:phenylalanine]·4Cl	0.8–2.6[a]	[**3**:phenyl α-D-glucoside]·4Cl	4.3[c]
[**3**:dopamine]·4Cl	3.8[a]	[**3**:phenyl β-D-galactoside]·4Cl	5.3[c]
[**3**:norepinephrine]·4Cl	4.0[a]	[**3**:phenyl α-D-mammoside]·4Cl	1.5[c]
[**3**:epinephrine]·4Cl	3.5[b]		

[a] $\Delta G°$ values were determined in 50 mM phosphate buffer.
[b] $\Delta G°$ values were determined in 1 M HCl.
[c] $\Delta G°$ values were determined in aqueous buffer (pH 7.4).

phane-like manner by means of two *p*-phenylene groups.[12a]

The-solid state structure of [**3**:**4c**]·4PF$_6$, whose symmetry is imposed by its $P[\bar{1}]$ space group, reveals (Figure 4) that the neutral substrate **4c** is threaded centrosymmetrically through the centre of the tetracationic cyclophane with interplanar separations between the π-electron-rich and the π-electron-deficient aromatic rings of *ca* 3.5 Å. The tilt of the O—C_6H_4—O axis of the substrate with respect to the N^+—N^+ vector in the tetracationic receptor is 52°. The separation between the oxygen atoms in the substrate and the proximal formally charged nitrogen atoms in the receptor ranges from 3.3 to 4.4 Å, indicating strong electrostatic interactions between the two components. These interactions are confirmed by the results of the binding studies between **3**·4PF$_6$ and **4a**–**e** (Table 2).

By comparing the free energies of complexation ($\Delta G°$) in MeCN corresponding to the complexes [**3**:**4a**–**e**]·4PF$_6$[13a] (Table 2), we observe that a maximum is quickly reached at **4c**, where diethylene glycol units are the appendages, suggesting that little further stabilization is provided when the polyether chain is longer.

On replacing the π-electron-rich core of the substrate with disubstituted dioxynaphthalene ring systems and retaining diethylene glycol units as the side-chains (**4f**–**i**)[10c], large differences in $\Delta G°$ values were observed. These values vary from -3.1 to -5.1 kcal mol^{-1}, leading us to the conclusion that once again, the substitution pattern on the dioxynaphthalene unit affects dramatically the molecular recognition event. The introduction of a carbonyl group into one of the polyether chains[13b] of the π-electron rich acyclic derivative (**4j**–**l**) decreases the $\Delta G°$ value from -4.9 to -3.9 kcal mol^{-1}. The introduction of a second carbonyl group into the other polyether chain brings about a decrease

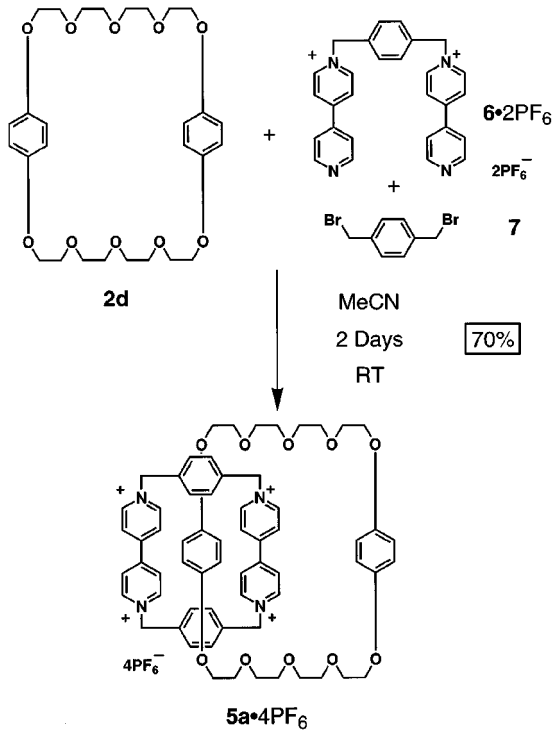

Scheme 1. Self-assembly of the [2]catenane **5a**·4PF$_6$

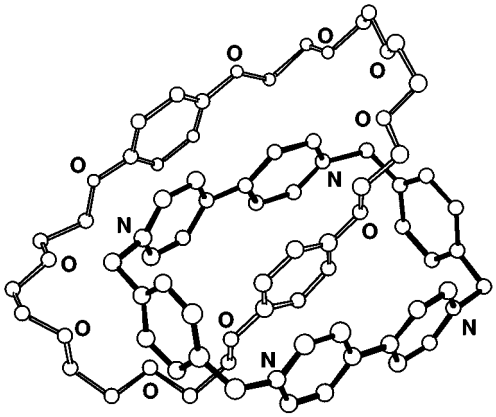

Figure 5. Ball-and-stick representation of the solid-state structure of the [2]catenane **5d**$^{4+}$

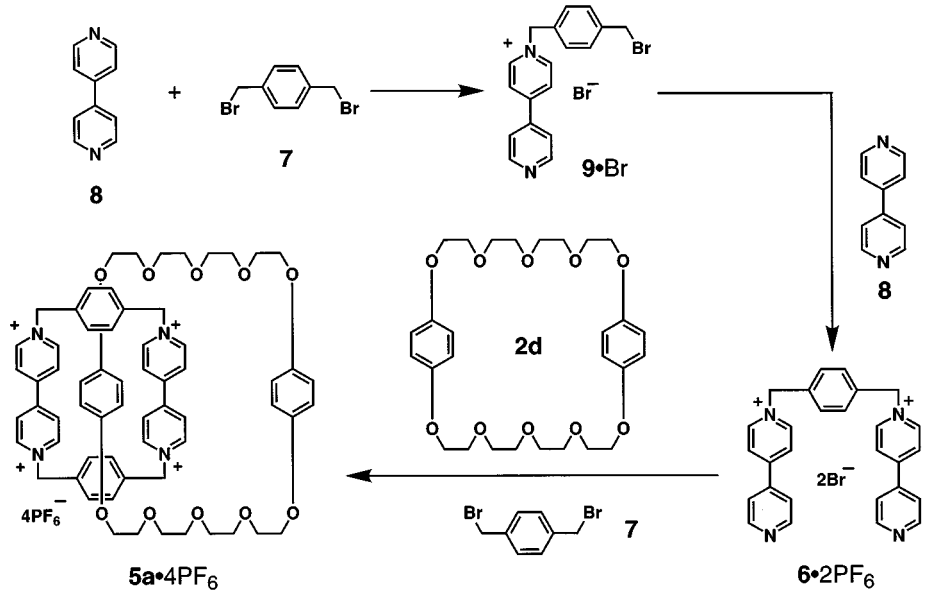

Scheme 2. Synthetic pathway for the self-assembly of the [2]catenane **5a**·4PF_6

of the association energy from -3.9 to -3.7 kcal mol^{-1}. Thus, the presence of the carbonyl group has a dramatic effect upon the recognition process—probably by decreasing the strength, via a combination of adverse steric and electronic effects as well as solvation factors, of the hydrogen bonding interactions between the acidic α-protons on the bipyridinium units and the oxygen atoms of the two polyether chains. In aqueous solution, cyclobis(paraquat-*p*-phenylene), as a tetrachloride salt **3**·4Cl, is a very efficient receptor (Table 3) for amino acids such as tryptophan, tyrosine or phenylalanine possessing π-electron-rich aromatic subunits.[13c] Even stronger complexes in aqueous solution are formed between **3**·4Cl and some neurotransmitters, such as dopamine, norepinephrine, epinephrine or serotonin.[13d] Furthermore, **3**·4Cl exhibits very selective complexation with some monosaccharide derivatives; it can discriminate, for example, between α- and β-diastereoisomers of phenyl D-glucoside (Table 3), presumably as a consequence of steric and/or solvation factors.[13e]

The near perfect match between the π-electron-rich substrates and the tetracationic cyclophane **3**·4PF_6 led us to improve the synthesis of the receptor by incorporating a π-electron-rich template, such as **4c**, in the reaction mixture.[12b] In this way, the yield of formation of **3**·4PF_6 has been improved from 12% without a template to 45% in the presence of **4c**, and to 62% at 12 kbar.

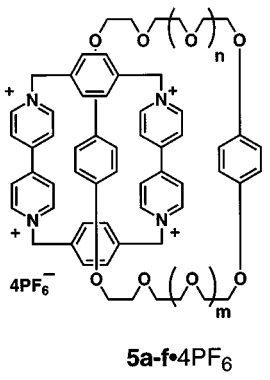

[2]Catenane	5a	5b	5c	5d	5e	5f
m	2	2	3	3	4	4
n	2	1	2	3	3	4
Yield (%)	70	10	55	54	40	49

Figure 6. Efficiency of the self-assembly of a range of [2]catenanes **5a**–**f**·4PF_6 as a function of the size of the macrocyclic polyether component

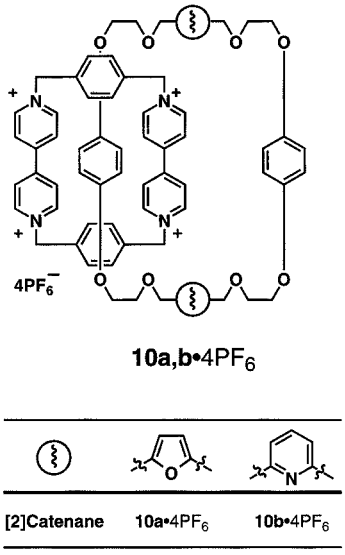

Figure 7. The catenanes **10a**·4PF_6 and **10b**·4PF_6 incorporating furan-2,5-dimethylenedioxy and pyridine-2,6-dimethylenedioxy residues in their macrocyclic polyether components, respectively

Synthesis and properties of self-assembling catenanes

The formation of 1:1 complexes between paraquat **1**·2PF_6 and **2d**, as well as between **3**·4PF_6 and **4c**, with a pseudorotaxane-like geometry in both solution and the solid state led us to the self-assembly of the [2]catenane **5a**·4PF_6, composed of the interlocked crown ether **2c** and the tetracationic cyclophane **3**·4PF_6, in 70% yield (Scheme 1).[14a]

The solid-state molecular structure of the [2]catenane **5a**·4PF_6 (Figure 5) turned out to be just as one might have predicted from the range of crystal structures of complexes formed between the mutually compatible components. As expected, one hydroquinone ring is incorporated in the centre of the tetracationic cyclophane and shows the same π–π stacking and T-type interactions as present in the complexes [**3**:**4a–l**]·4PF_6. Moreover, hydrogen bonds are observed between the acidic hydrogen atoms in the α-position of the bipyridinium units and the polyether oxygen atoms of the crown ether component. The separation between the mean planes of the π-electron-deficient and π-electron-rich aromatic units is again *ca* 3.5 Å, not only within the molecule but also supramolecularly along the polar stack (see below).

Investigation of the mechanism of formation of the [2]catenane **5a**·4PF_6 has been carried out by ^{1}H NMR spectroscopy in order to elucidate the reaction pathway and characterize the intermediates present in the self-assembly process.[14b] This study revealed that, when the starting materials were **7** and **8**, the monocation **9**$^+$ and the dication **6**$^{2+}$ were stable intermediates (on the NMR time-scale) involved in the reaction pathway (Scheme 2).

In order to probe the efficiency of this self-assembly procedure, several analogues of the [2]catenane **5a**·4PF_6 have been synthesized and studied. It is of interest to compare the yields of formation of similar [2]catenanes since they reflect the information present within their molecular components. A list of yields for the formation of the [2]catenanes **5b–f**·4PF_6, in which the polyether chains have been lengthened or shortened, is provided in Figure 6.[15a] As expected from the free energies of complexation (Table 1), the highest yield was achieved when the crown ether **2d** was the template since the cavity of the crown ether **2c** is too small to allow the efficient complexation of a bipyridinium unit; the self-assembly of the corresponding [2]catenane **5b**·4PF_6 occurs in a yield of only 10%. As the dimensions of the crown ether component are increased, the yield of the [2]catenanes **5d–f**·4PF_6 decreases, in line with the trend suggested by the free energies of complexation ($\Delta G°$) for paraquat **1**·4PF_6 and the crown ethers **2e–f** (Table 1).

Replacement of the central oxygen atom of the polyether

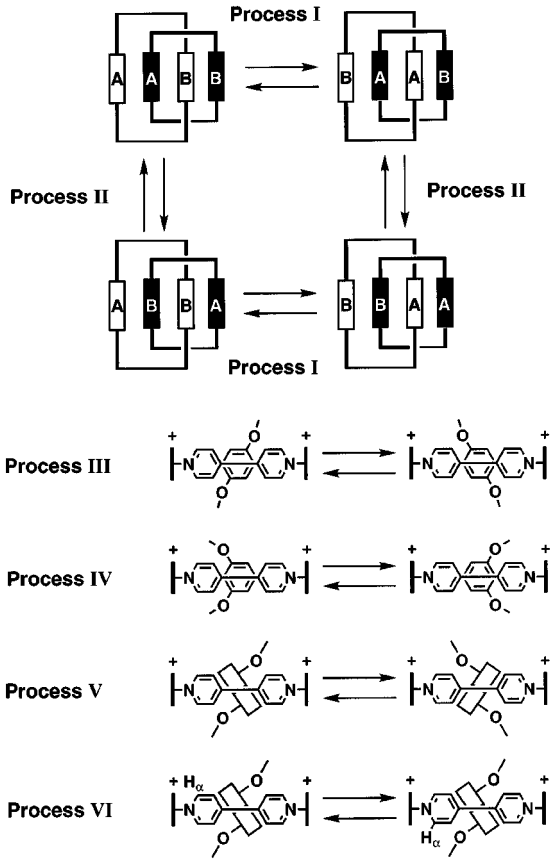

Scheme 3. The various dynamic processes which can be observed by dynamic ^{1}H NMR spectroscopy in solution for the [2]catenanes **5a**,**g–s**·4PF_6

Table 4. Free energies of activation associated with the various dynamic processes occurring in the [2]catenanes **5a**,**g**–**s**·$4PF_6$

Compound	Crown ether component: Aromatic unit 1[a]	Crown ether component: Aromatic unit 2[b]	Yield (%)	$-\Delta G_c^{\ddagger}$(I)[c] (kcal mol^{-1})	$-\Delta G_c^{\ddagger}$(II)[d] (kcal mol^{-1})	Process/$-\Delta G_c^{\ddagger}$[e] (kcal mol^{-1})
5a·$4PF_6$	HQ	HQ	70	15.6[f]	12.0[f]	III/9[f]
5g·$4PF_6$	HQ	Res	15	15.4[f]	11.1[f]	
5h·$4PF_6$	Res	Res	17	13.6[f]		IV/12.2[f]
5i·$4PF_6$	HQ	1/6DN	82		11.2[f]	III/8.5[f]
5j·$4PF_6$	HQ	2/6DN	89		11.4[f]	
5k·$4PF_6$	HQ	2/7DN	74		11.9[f]	III/10.6[f]
5l·$4PF_6$	1/5DN	1/5DN	51	17.2[g]	12.7[g]	V, VI/15.8[g]
5m·$4PF_6$	1/6DN	1/6DN	35	13.5[g]	9.8[g]	
5n·$4PF_6$	2/6DN	2/6DN	16	14.4[g]	11.4[g]	V,VI/12.8[g]
5o·$4PF_6$	2/7DN	2/7DN	27	13.9[f]	8.9[f]	V, VI/11.8[f]
5p·$4PF_6$	1/5DN	1/6DN	64	15.4[g]	11.1[f]	V, VI/15.4[g]
5q·$4PF_6$	1/5DN	2/6DN	74	16.7[g]	11.7[f]	V, VI/16.7[g]
5r·$4PF_6$	1/5DN	2/7DN	84	16.7[g]	11.5[f]	V, VI/16.7[g]
5s·$4PF_6$	2/6DN	2/7DN	25	13.2[f]	11.0[f]	V, VI/16.7[f]

[a] One of the two aromatic units of the crown ether component arbitrarily chosen as number 1.
[b] One of the two aromatic units of the crown ether component arbitrarily chosen as number 2.
[c] Free energies of activation associated with process I (Scheme 3).
[d] Free energies of activation associated with process II (Scheme 3).
[e] Free energies of activation associated with process III, IV or V and VI.
[f] Determined in CD_3COCD_3.
[g] Determined in CD_3CN.

chain of the crown ether component with both furan-2,5-diyldimethylenedioxy[15b] and pyridine-2,6-diyldimethylenedioxy[8c] residues has allowed us to assess the significance of the [C—H · · · O] hydrogen bonds in the self-assembly process leading to the formation of the [2]catenanes **10a**·PF_6 and **10b**·$4PF_6$ (Figure 7). It appears that enhanced rigidity of the polyether chain, on account of the incorporation of the furan or the pyridine rings, significantly lowers the yields of the [2]catenanes **10a**·$4PF_6$ and **10b**·$4PF_6$ to 40% and 31%, respectively.

The information responsible for the formation of the bipyridinium-based [2]catenanes 'lives on' in their molecular structures and gives rise to a variety of dynamic processes (Scheme 3). It has been possible, in many cases, to determine the energies of activation associated with these dynamic processes by variable-temperature ^{1}H NMR spectroscopy using the coalescence[16a] or the linewidth[16b] approximate treatments. In order to understand and possibly control the dynamic processes occurring between the two interlocked rings, [2]catenanes in which the aromatic units of the crown ether component have been modified to incorporate resorcinol[17] and dioxynaphthalene units[10c] have

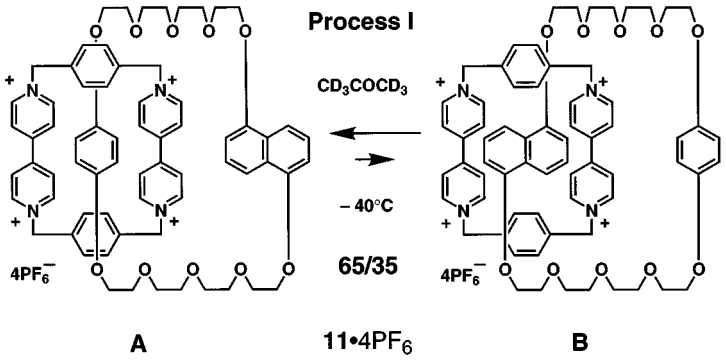

Scheme 4. Equilibration of translational isomers for the [2]catenane **11**·$4PF_6$ at -40 °C in CD_3COCD_3

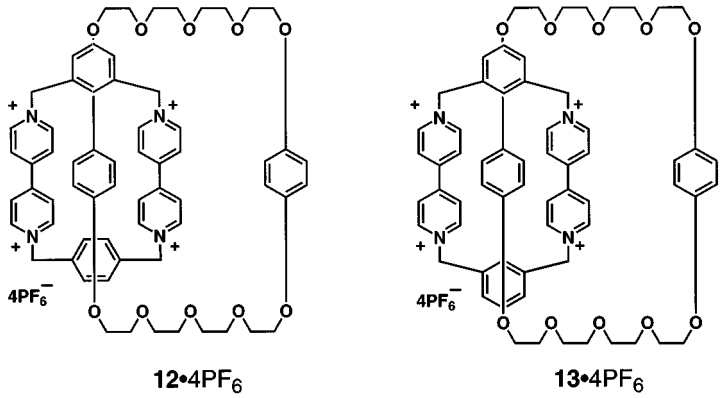

12•4PF$_6$ **13**•4PF$_6$

Figure 8. The [2]catenanes **12**·4PF$_6$ and **13**·4PF$_6$ in which the tetracationic cyclophane component contains two bipyridinium units bridged by one or two *m*-xylyl spacers, respectively

been synthesized in moderate to good yields (Table 4).

The two dynamic processes associated with the highest energies of activation ($\Delta G_c\ddagger$) occurring in [2]catenanes (processes I and II in Scheme 3) involve the exchange of the π-electron-rich ring systems in the crown ether (process I), and the exchange of the π-electron-deficient units in the tetracationic cyclophane (process II), between 'inside' and 'alongide' environments. The $\Delta G_c\ddagger$ values, associated with process I in the [2]catenanes **5a,g,l,p**–**r**·4PF$_6$, reflect the high affinities of the tetracationic cyclophane component for any crown ether component which contains a hydroquinone ring and/or a 1,5-dioxynaphthalene ring system. The same trend is observed for the free energies of activation associated with process II. Another interesting phenomenon, directly associated with these two processes, is the presence in solution of two translational isomers (Scheme 4) when the crown ether moiety contains two different aromatic residues.

In the case of the [2]catenane **11**·4PF$_6$ (Scheme 4), the ratio of isomers[18] is 65:35 (**A**:**B**) in CD_3COCD_3 at -40 °C, when, according to the free energies of complexation estimated between **3**·4PF$_6$ and **4c** and **4i** (Table 2), we could have expected an opposite ratio. Moreover, the solvent dielectric and the ratios of the translational isomers exhibit a sigmoidal relationship that can be explained if we consider that translational isomerism is a delicate balance between π–π stacking and solvation. We believe that the tetracationic cyclophane component favours a shielding situation in relatively non-polar solvents, such as CD_3COCD_3. The larger π-electron-donating surface areas associated with the 1,5-dioxynaphthalene residue therefore resides preferably on the outside of the tetracationic cyclophane, favouring isomer **A** (Scheme 4).

A third dynamic process (process III in Scheme 3) was observed,[10c] with a much lower energy of activation, in some [2]catenanes in which the crown ether component

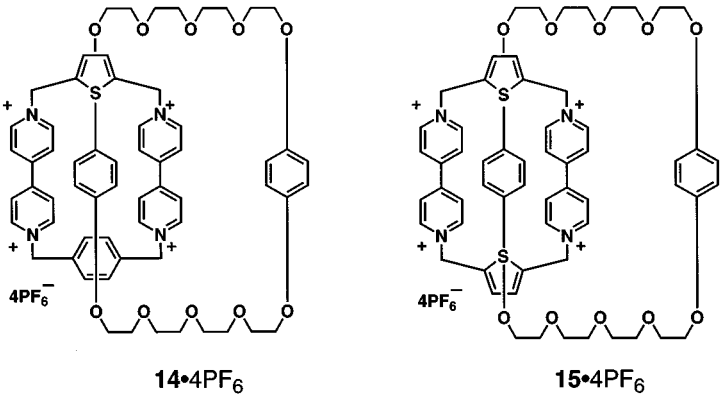

14•4PF$_6$ **15**•4PF$_6$

Figure 9. The [2]catenanes **14**·4PF$_6$ and **15**·4PF$_6$ in which the *p*–xyxlyl spacers of the tetracationic cyclophane component have been replaced by one and two 2,5-disubstituted thiophene units, respectively

incorporates a hydroquinone ring (**5i**,**k**·4PF_6, Table 4). It has been found that the free energy of activation (ΔG_c‡) associated with this process ranges from 8.5 to 10.6 kcal mol^{-1}. In the case of the [2]catenane **5h**·4PF_6, in which the crown ether component incorporates two resorcinol rings,[17] a fourth dynamic process (process IV in Scheme 3) occurs, corresponding to the dislocation of the resorcinol ring from the cavity of the tetracationic cyclophane, followed by its reorientation and return inside the cavity. The free energy of activation of 12.1 kcal mol^{-1} governing this process is slightly lower than that (ΔG‡ = 13.6 kcal mol^{-1}) required for a complete exchange of two resorcinol rings with respect to the cavity of **3**·4PF_6.

Other processes (processes V and VI in Scheme 3) can take place when the crown ether component of the [2]catenane contains a dioxynaphthalene ring system.[10c] The highest energy process (process V in Scheme 3) is the dislocation of the dioxynaphthalene unit from within the cavity of the tetracationic cyclophane and its rotation about its O · · · O axis before it re-enters the cavity. The lowest energy process (process VI in Scheme 3) is the rotation of the bipyridinium units about their N · · · N axes, whilst the dioxynaphthalene ring system departs at least partially from the cavity of the tetracation. These two processes (V and VI) possess similar coalescence temperatures at 400 MHz and, therefore the free energies of activation that are reported in Table 4 correspond to an averaged process involving processes V and VI. Values of the free energies of activation for Processes V and VI are high (11.8–16.7 kcal mol^{-1}) compared to those associated with other processes and they show how tightly bound a dioxynaphthalene ring system is within the cavity of the tetracationic cyclophane **3**·4PF_6.

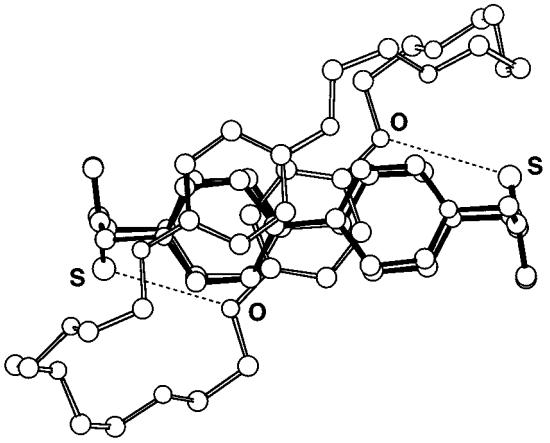

Figure 10. Ball-and-stick representation of the side view of the solid-state structure of the [2]catenane $\mathbf{15}^{4+}$ illustrating the short oxygen–sulphur interaction

Replacement of the spacer *p*-xylyl between the two bipyridinium units of the tetracationic component in the [2]catenane by either a *m*-xylyl[19] or a thiophene-2,5-diyldimethylenedioxy residues[20] has been achieved in an effort to gain insight into the effects of such changes upon the dynamic processes (Figures 8 and 9). Indeed, when the *p*-xylyl spacers of the tetracation were replaced by one and then two *m*-xylyl spacers,[19] the free energies of activation associated with process I (Scheme 3) are increased from 15.6 kcal mol^{-1} in **5a**·4PF_6 to 16.3 kcal mol^{-1} in **12**·4PF_6 and then to 17.6 kcal mol^{-1} in **13**·4PF_6.

When the *p*-xylyl spacers were replaced by one and then by two thiophene-2,5-diyldimethylenedioxy residues,[20] the free energies of activation for processes I and II were approximatively the same as in **5a**·4PF_6. A significant increase in the energy associated with process III (Scheme 3) from 9.0 kcal mol^{-1} in **5a**·4PF_6 to 9.7 kcal mol^{-1} in **14**·4PF_6 and 10.8 kcal mol^{-1} in **15**·4PF_6 was observed. The x-ray crystal structure (Figure 10) of **15**·4PF_6 offers some insight into this phenomenon since it shows that there is a significant [S · · · O] interaction between the sulphur atom

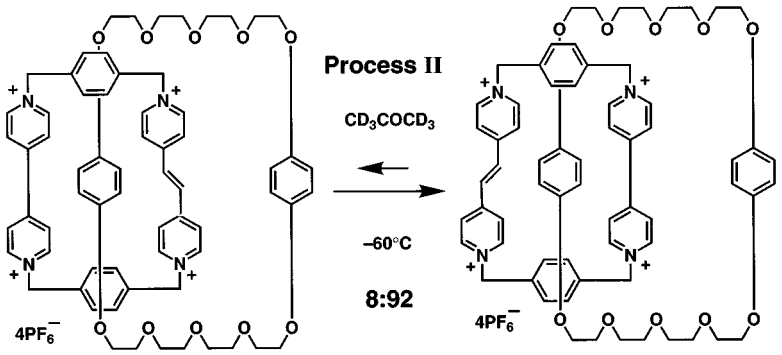

Scheme 5. Equilibration of translational isomers for the [2]catenane **16**·4PF_6 at − 60 °C in CD_3COCD_3

in the spacer groups of the tetracationic cyclophane component and the oxygen atoms of the included hydroquinone ring in the neutral component (the [S · · · O] distances are 3.24 and 3.27 Å; this [S · · · O] interaction is rather unique, since there are no reports, to our knowledge, of such interactions).

The last subcomponent that has been modified, in order to complete the study of the influence of all the components upon the self-assembly processes, is the π-electron-deficient bipyridinium unit of the tetracationic cyclophane component. This modification was achieved by replacing the bipyridinium rings with one or two π-extended viologen units[21,22] with the aim of controlling the translational isomerism exhibited by these structures. For example, in the case of the [2]catenane **16**·4PF$_6$ (Scheme 5), the polyether macrocycle component prefers[21] to encircle the bipyridinium unit rather than the π-extended viologen unit at − 60 °C in CD_3COCD_3, resulting in an 8:92 ratio for **C**:**D**.

In the case of **17**·4PF$_6$,[22] where all the π-electron-deficient and the π-electron-rich components are different, four distinct translational isomers can co-exist in solution (Scheme 6). At room temperature, when process I is fast and process II is slow on the ^{1}H NMR time-scale, we observed, by ^{1}H NMR spectroscopy in CD_3COCD_3, the presence of the isomers in which either the 1,5-dioxynaphthalene ring system or the hydroquinone ring occupies the cavity of the tetracationic cyclophane in a ratio of 88:12, respectively. At − 40 °C, in the same solvent, when processes I and II are both slow on the NMR time-scale, we observed only two of the four possible translational isomers in which the dioxynaphthalene unit is located inside the cavity of the charged component in a 95:5 ratio. At that temperature, the most favoured isomer is the one in which the bipyridinium unit occupies the cavity of the crown ether component. This isomer corresponds to that observed in the solid state for **17**·4PF$_6$.

The self-assembly paradigm has been employed[23,24] in the template-directed syntheses of [3]-, [4]- and [5]catenanes. By enlarging the tetracationic component in an appropriate manner, we were able to entrap simultaneously two polyether macrocycles (Scheme 7), and by so doing we obtained[23] the [3]catenanes **18**·4PF$_6$ and **19**·4PF$_6$ in 25 and 30% yields, respectively. The only dynamic process observed in these [3]catenanes is the exchange of the aromatic residues of the crown ether component. The free energies of activation associated with this process are

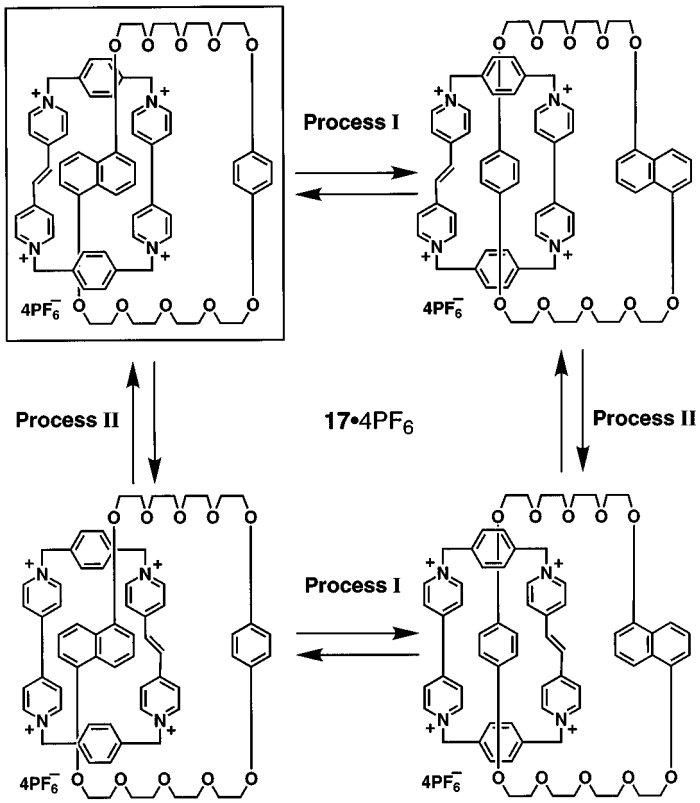

Scheme 6. Equilibration of translational isomers for the [2]catenane **17**·4PF$_6$ in solution

10.7 kcal mol^{-1} in **18**·4PF$_6$ and 13.3 kcal mol^{-1} in **19**·4PF$_6$.

The [3]catenane **20**·4PF$_6$, containing a large neutral macrocyclic polyether component—self-assembled in 6% yield in the same way as **18**·4PF$_6$ and **19**·4PF$_6$—was further reacted (Scheme 8) with **7**·2PF$_6$ and **6**·2PF$_6$ to afford[24] the [4]- and [5]catenanes **21**·8PF$_6$ and **22**·12PF$_6$ in yields of 31 and 5%, respectively. The [5]catenane **22**·12PF$_6$, which we have dubbed 'olympiadane' following van Gulick's original suggestion, was fully characterized on the basis of mass spectrometric and ^{1}H NMR spectroscopic data. From ^{1}H NMR experiments, a value for the free energy of activation necessary to dislodge the dioxynaphthalene ring systems from the cavity of the smaller tetracationic cyclophane in **22**·12PF$_6$ was determined to be 14.7 kcal mol^{-1}, a value consistent with those obtained for processes V and VI in **5l**,**n**–**s**·4PF$_6$.

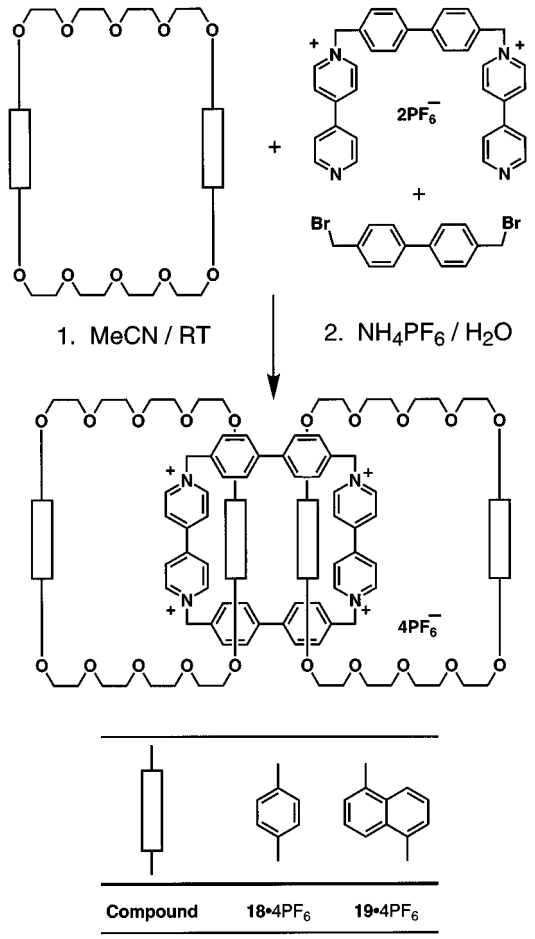

Scheme 7. Self-assembly of two [3]catenanes, **18**·4PF$_6$ and **19**·4PF$_6$, incorporating a cyclobis(paraquat-4,4′-biphenylene) as the tetracationic cyclophane component

Solid-state structures and superstructures

We have shown that the recognition even between π-electron-rich and π-electron-deficient motifs is a very powerful tool in the self-assembly process as it occurs in solution. In crystals, which are supramolecular arrays *par excellence*, the solid-state structures of the assemblies we have considered so far not only give us precious structural information about non-covalent bonding interactions, but they also reveal that the information responsible for the self-assembly of the catenanes and their dynamic behaviour in solution extends beyond the molecule to form highly ordered one-, two- or three-dimensional arrays in the solid state.[25]

The solid-state structure (Figure 11) of the tetracationic cyclophane **3**·4PF$_6$, reveals[26] that each macrocycle ring is stacked almost directly above its neighbour (by a unit lattice translation of *ca* 11.01 Å) with four PF_6^- counterions and two MeCN molecules forming a torus so that the overall solid-state structure contains parallel open channels bounded by alternately charged ($4^+/4^-$) entities. A third MeCN molecule is located in part of the void created by these channels.

It has been possible to include π-donor guests, such as TTF[27] (Figure 12) and even the bis-1,5-dioxynaphthalene derivative **23** (Figure 13), inside the channels formed by the tetracationic cyclophane, without altering the channel structure of the tetracation.[28] In the solid state, the 1:1 complex formed between TTF and **3**·4PF$_6$ features[27] continuous one-dimensional stacks (Figure 12) with no hindrance of the central channel by either an MeCN molecule or a PF_6^- counterion. The TTF molecules have their long axes almost perfectly aligned with a separation of 4.87 Å between the endocyclic olefinic carbon atoms in adjacently located TTF molecules. The solid-state structure (Figure 13) of the 2:1 complex formed between **23** and **3**·4PF$_6$, reveals[28] the commensurate nature of their arrangement in the solid state, the chief geometric requirements being that the dioxynaphthalene units lie within the centre of the tetracationic cyclophane and that the polyether chain possesses the same length as the interchannel separation.

Compound **24**·2PF$_6$ is a dicationic cyclophane (Figure 14) which contains a π-electron-deficient bipyridinium unit that is positioned parallel with respect to a π-electron-rich hydroquinone ring.[29] The solid-state structure of **24**·2PF$_6$ reveals that, within each molecule, the hydroquinone ring is positioned in a π–π stacking manner with respect to the bipyridinium unit, their interplanar separation being *ca* 4.0 Å. The O · · · O axis of each hydroquinone ring is skewed with respect to the $N^+ \cdots N^+$ axis of its associated bypiridinium unit, producing a geometry very similar to that observed (Figures 2, 4 and 5) in other supramolecular systems containing these two components.

Furthermore, the dications are stacked such that the bipyridinium unit of one molecule inserts itself into the cleft formed by the inwardly folded hydroquinone ring of another to form an extended π-donor–π-acceptor stack, the inter-

molecular interplanar separation being 3.7 Å. An investigation of the solid-state structure of the 1:2 complex formed (Figure 15) between the macrocyclic polyether **2j** and paraquat **1**·2PF_6 has revealed[10c] the formation of a very similar continuously stacked π-donor–π-acceptor structure with paraquat dications alternatively included within and sandwiched between adjacent macrocycles. A paraquat dication is sandwiched within the macrocycle between the parallel-aligned dioxynaphthalene residues and is oriented so as to maximize overlap with the two π-electron-rich residues. The second paraquat dication is positioned between adjacent inclusion complexes and nearly perfectly coaligned with its included counterpart. Similarly, the packing (Figure 16) in the solid-state structure of the [2]catenane **5l**·4PF_6 reveals[30] the existence of continuously stacked entities. The approximate interplanar separation between overlapping π-electron-rich and -deficient components in adjacently stacked catenane entities is *ca* 3.5 Å. In the last two examples, it is striking to note that there is no difference between interaction patterns determined by intramolecular assembly and crystal packing.

Interestingly, the ordering within the solid state structure (Figure 17) of the [3]catenane **18**·4PF_6 shown in Scheme 7 reveals[23] the loss of the alternating pattern of π-donors (D) and π-acceptors (A) that was observed in the previous case in the [2]catenane **5l**·4PF_6. More surprisingly, however, this DADDAD sequence extends beyond the molecule throughout the crystal, producing (Figure 17) a continuously stacked array.

The tetracationic cyclophane **25**·4PF_6 packs (Figure 18) to form mosaic-like two-dimensional arrays in the crystal.[13b] In one direction, the bipyridinium units of adjacent molecules are unexpectingly aligned in register and separated by an interplanar distance of *ca* 3.7 Å. In the other direction, the biphenylene units are offset such that only one of the two phenylene rings overlaps with another phenylene ring in the adjacent molecule, the inter-ring plane separation being 3.4 Å.

In the solid state (Figure 19), the [2]pseudorotaxane [**3**:**26**]·4PF_6 not only has the acyclic polyether **26** inserted through the centre of the tetracation $\mathbf{3}^{4+}$, such that the middle 1,5-dioxynaphthalene unit is enriched,[31] but its polyether chains also curl back on themselves around the cyclophane, enabling the other two π-donors to stack against the sides of the π-accepting bipyridinium units. In the crystal lattice, the [2]pseudorotaxanes are arranged to form infinite two-dimensional sheets, sustained by a combination of aromatic π–π stacking and [CH · · · π]

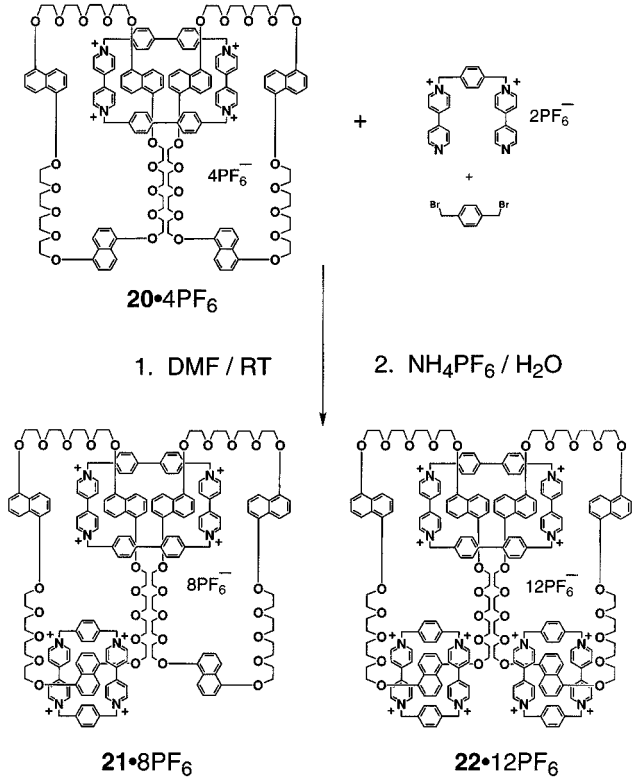

Scheme 8. Self-assembly process leading to the [4]catenane **21**·8PF_6 and the [5]catenane **22**·12PF_6

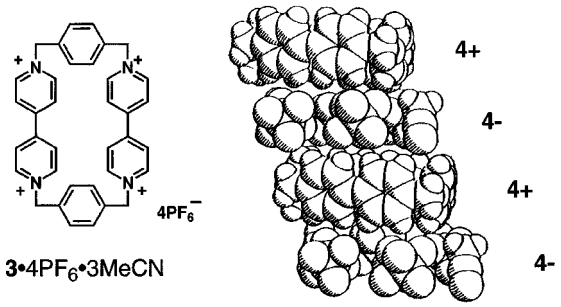

Figure 11. Space-filling representation of the alternatively charged entities of **3**·4PF_6·3MeCN in the solid state

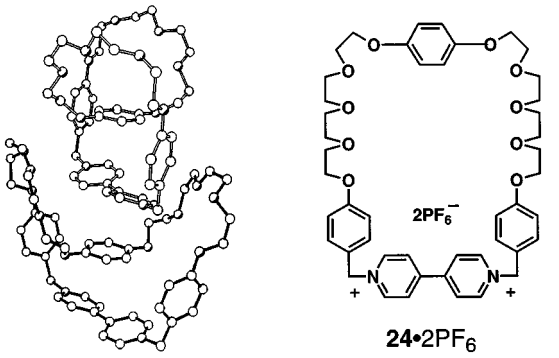

Figure 14. Ball-and-stick representation of the stacking of two crystallographically independent forms of $\mathbf{24}^{2+}$

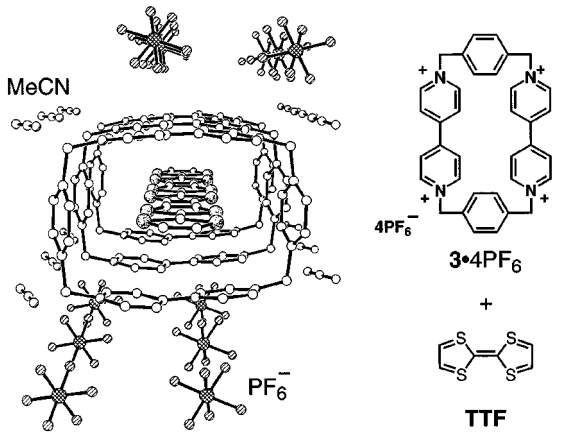

Figure 12. Part of one of the continuous stacks of [**3**:TTF:4MeCN]·4PF_6 in the solid state

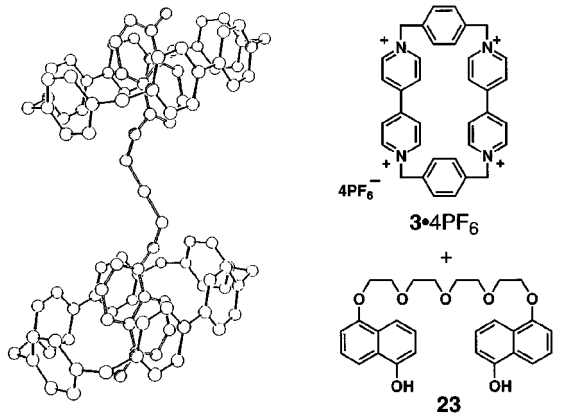

Figure 13. Ball-and-stick representation of the solid-state structure of the 2:1 complex $[(\mathbf{3})_2{:}\mathbf{23}]^{4+}$

interactions that extend within and between the 1:1 complexes to create a grid-like pattern.

Similarly, the solid-state structure (Figure 20) of the [2]catenane **27**·4PF_6 reveals[32] a highly ordered arrangement in which one dioxynaphthalene ring system is sandwiched between the two bipyridinium units in the tetracation. The other two dioxynaphthalene ring systems are positioned with one 'alongside' one of the bipyridinium units, and the other one adjacent to one of the *p*-xylyl spacers in the tetracationic cyclophane. The π-donor–π-acceptor inter-

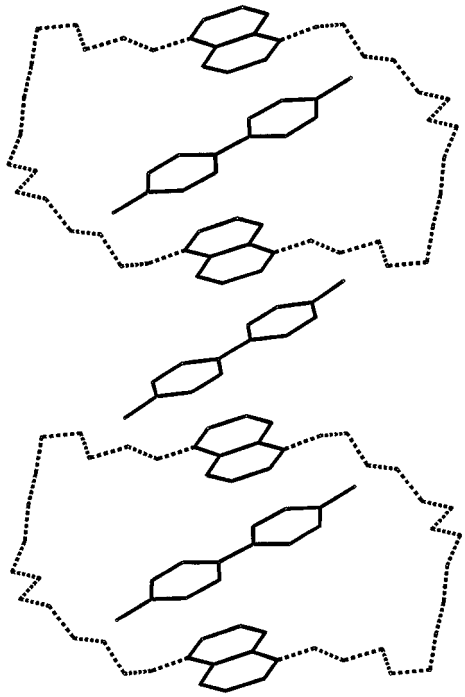

Figure 15. Part of the continuous π-donor–π-acceptor stack in the 2:1 crystalline complex represented by $[(\mathbf{1})_2{:}\mathbf{2j}]^{4+}$

actions present within the molecule extend in two orthogonal directions in the crystal to form a two-dimensional quilt-like array of [2]catenanes involving all of the aromatic rings.

The self-complementary cyclophane **28**·4PF_6 has been designed[33] in such a way that it can express itself

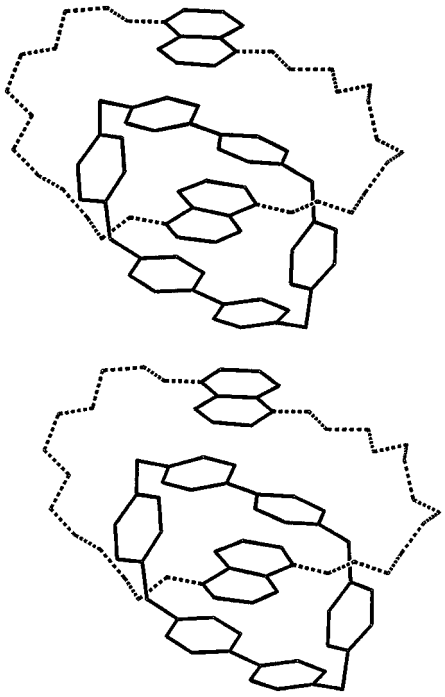

Figure 16. Part of the continuous π-donor–π-acceptor stack associated with the [2]catenane **5l**$^{4+}$ in the crystal

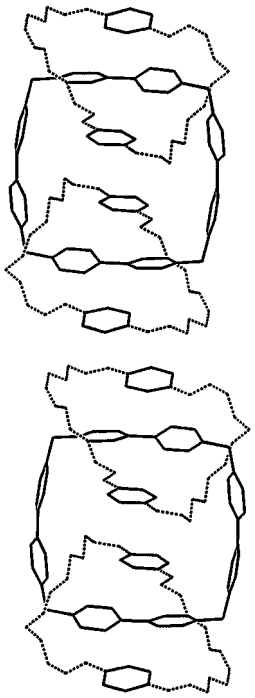

Figure 17. Stacked DADDAD–DADDAD superstructure of the [3]catenane **18**$^{4+}$

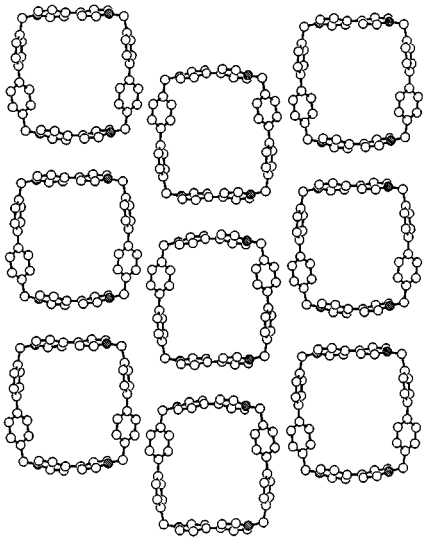

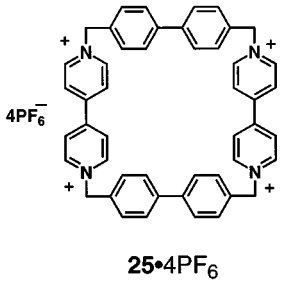

Figure 18. Ball-and-stick representation of one of the layers of the cyclophane **25**$^{4+}$ in the solid state

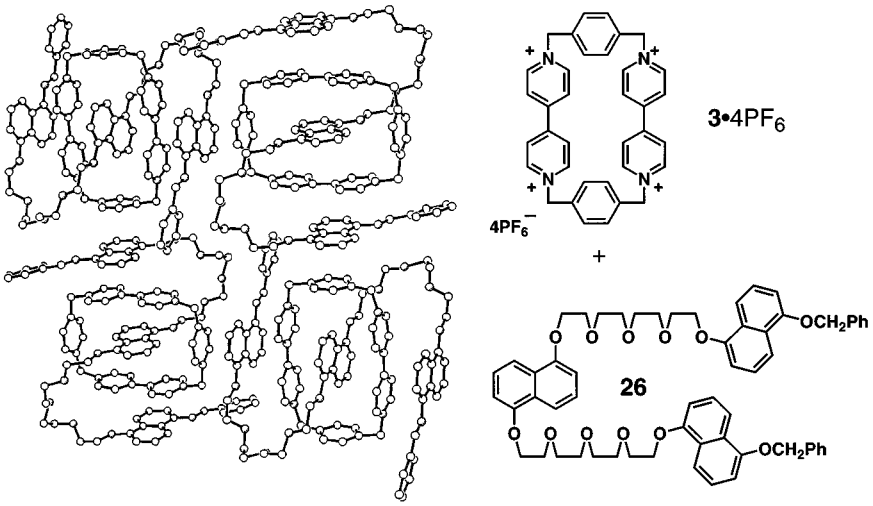

Figure 19. Part of the continuous two-dimensional π–π stacks formed by the [2]pseudorotaxane [**3**:**26**]$^{4+}$

simultaneously as both an *exo* and an *endo* receptor. The incorporation of two hydroquinone rings and two bipyridinium units in diametrically opposed positions gives **28**$^{4+}$ the potential to form a highly structured two-dimensional array (Figure 21) of stacked π-donor–π-acceptor systems after a mosaic-like fashion. A study of the packing (Figure 21) in the solid state of the tetracationic cyclophane **28**·4PF$_6$ reveals that an even more highly ordered two-dimensional π-donor–π-acceptor mosaic is present than is so in the case of **25**·4PF$_6$. Indeed, adjacent cyclophanes within one sheet retain proximal relationships between bipyridinium units in one tetracation and hydroquinone rings in the next and *vice versa*, thus allowing the tetracation to adopt a conventional π-donor–π-acceptor stack. The mean plane separation between these residues is 4.0 Å. Although adjacent sheets are separated by layers of disordered PF_6^- ions and MeCN molecules, the tetracations are in register and form channels (Figure 22) that extend throughout the crystal, the distance between the sheets being 9.8 Å. This superstructure is reminiscent of the one observed in the solid-state superstructure of the cyclophane **3**·4PF$_6$.[26]

Furthermore, the symmetrically oriented molecular rec-

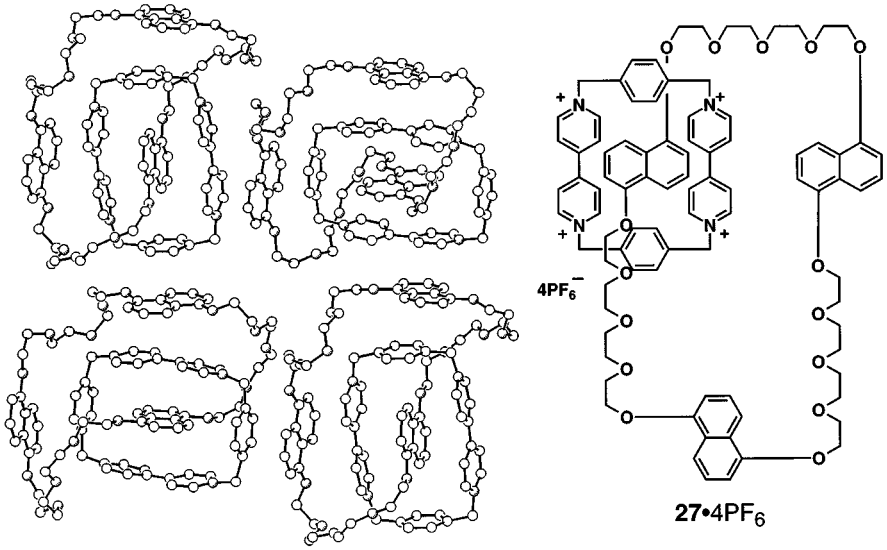

Figure 20. Part of the continuous two-dimensional π–π stacks formed by the [2]catenane **27**$^{4+}$

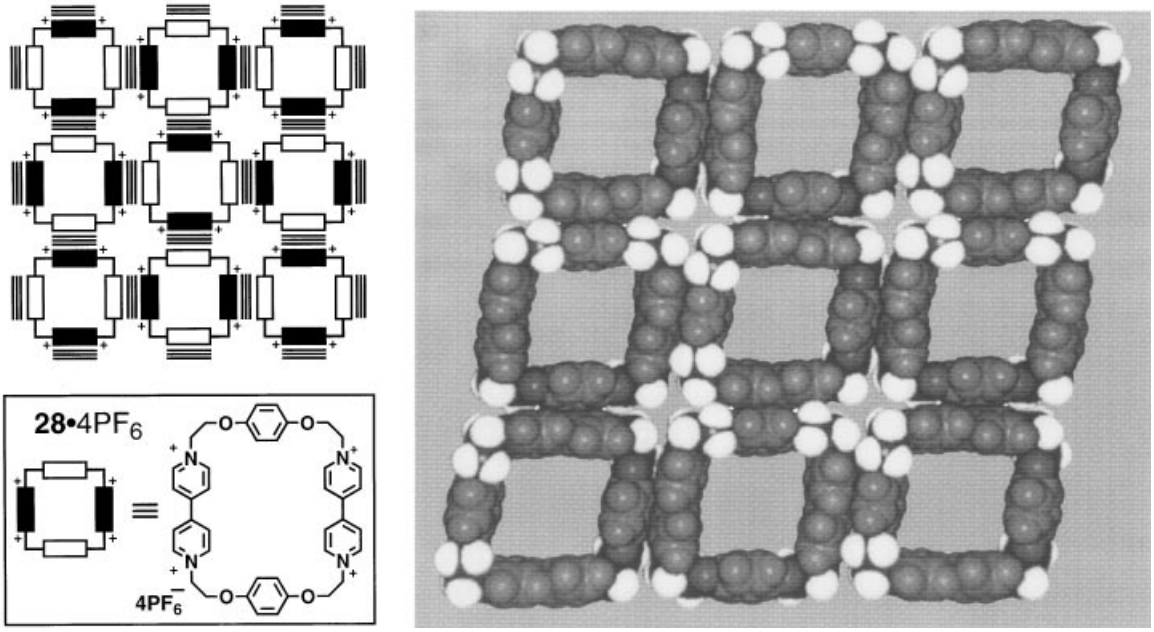

Figure 21. Space-filling representation of the packing of **28**·4PF$_6$ in the solid state

ognition elements of the tetracationic cyclophane **28**·4PF$_6$ have allowed the directionally specific inclusion of a ferrocene molecule (**Fc**) within its cavity to form the 1:1 adduct **28**/**Fc**·4PF$_6$ (Figure 23). The x-ray crystallographic analysis of **28**/**Fc**·4PF$_6$ reveals a C_i-symmetric adduct in which the cyclopentadienyl rings are sandwiched between the faces of the bipyridinium units. The packing of this 1:1 adduct is virtually identical with that of the free cyclophane **28**·4PF$_6$ (the mosaic-like structure and the channel structure are retained) with a slightly improved packing: the pyridinium–hydroquinone ring separations are reduced to 3.8 Å.

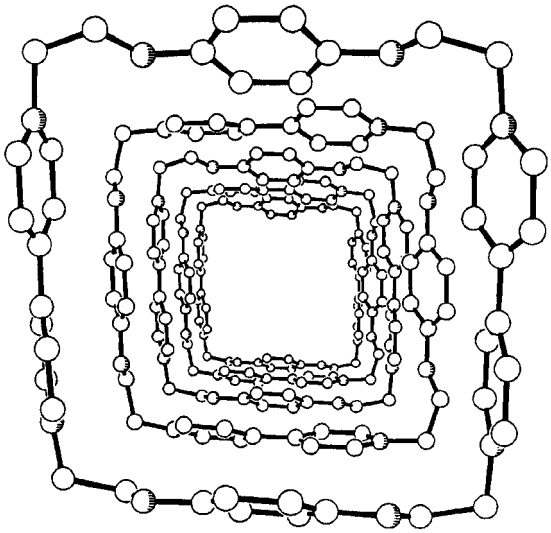

Figure 22. Ball-and-stick representation of the view down a channel of **28**$^{4+}$ ions in the solid state

CONCLUSION

In this short review, we have outlined the significance of π–π interactions in the building up of molecular assemblies and supramolecular arrays, employing the methodology of self-assembly. We have also came to appreciate that other weak noncovalent bonding interactions, such as [CH · · · O] hydrogen bonds or [CH · · · π] interactions, participate in a cooperative manner, leading to the successful realization of these structural and superstructural architectures. The data that we and others have accumulated over the years from solution-state investigations, and from the careful examination of the non-covalent interactions in the solid state, are now paving the way towards the design new molecular assemblies and supramolecular arrays which may prove valuable in the development of new materials and/or functioning devices.

ACKNOWLEDGMENTS

We thank Professor D. J. Williams of Imperial College London for determining the numerous x-ray crystal structures discussed in this review. We are grateful to the

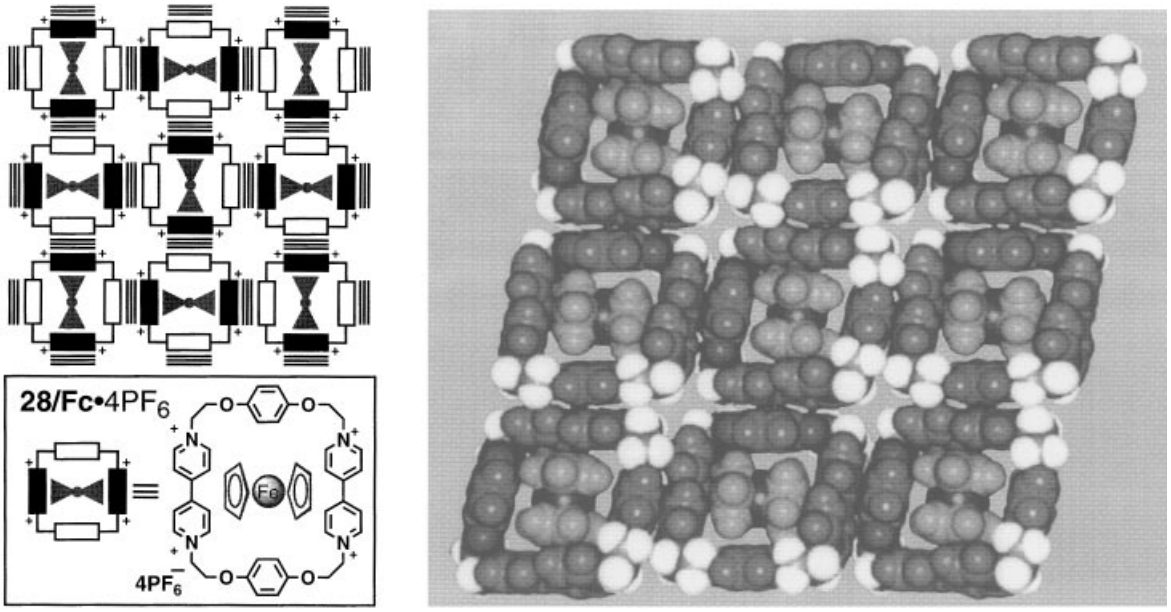

Figure 23. Space-filling representation of the packing of the 1:1 adduct **28**/Fc·4PF_6 between **28**·PF_6 and ferrocene in the solid state

Biotechnology and Biological Sciences Research Council and to the Engineering and Physical Sciences Research Council for their support of various research programmes at Birmingham. One of us (C.C.) thanks the Ministère de la Recherche et de l'Enseignement Supérieur, France, for financial support.

REFERENCES

1. (a) J. S. Lindsey, *New J. Chem.* **15**, 153–180 (1991); (b) G. M. Whitesides, J. P. Mathias and C. T. Seto, *Science* **254**, 1312–1319 (1991); (c) G. M. Whitesides, E. R. Simanek, J. P. Mathias, C. T. Seto, D. N. Chin, M. Mammen and D. M. Gordon, *Acc. Chem. Res.* **28**, 37–44 (1995); (d) D. S. Lawrence, T. Jiang and M. Levett, *J. Am. Chem. Soc.* **95**, 2229–2260 (1995); (e) D. Philp and J. F. Stoddart, *Synlett* 445–461 (1991); (f) D. B. Amabilino and J. F. Stoddart, *Chem. Rev.* **95**, 2725–2828 (1995); (g) D. Philp and J. F. Stoddart, *Angew. Chem., Int. Ed. Engl.* **35**, 1155–1196 (1996).
2. (a) R. Kramer, J. M. Lehn and A. Marquis-Rigault, *Proc. Natl. Acad. Sci. USA* **90**, 5394–5398 (1993); (b) E. C. Constable, *Angew. Chem., Int. Ed. Engl.* **30**, 1450–1451 (1991); (c) E. C. Constable, A. J. Edwards, P. R. Raithby and J. V. Walker, *Angew. Chem., Int. Ed. Engl.* **32**, 1465–1467 (1993); (d) E. C. Constable, M . J. Hannon, A. J. Edwards and P. R. Raithby, *J. Chem. Soc., Dalton Trans.* 2669–2677 (1994).
3. (a) P. J. Collings, *Liquid Crystals: Natures Delicate Phase of Matter.* Princeton University Press, Princeton, NJ (1990); (b) U. Kumar, T. Kato and J. M. J. Fréchet, *J. Am. Chem. Soc.* **114**, 6630–6639 (1992); (c) B. Xu and T. M. Swager, *J. Am. Chem. Soc.* **115**, 1159–1160 (1993); (d) R. Atencio, J. Barbera, C. Cativiela, F. J. Lahoz, J. L. Serrano and M. M. Zurbano, *J. Am. Chem. Soc.* **116**, 11558–11559 (1994).
4. (a) G. R. Desiraju, *Crystal Engineering: the Design of Organic Solids.* Elsevier, Amsterdam (1987); (b) M. C. Etter, Z. Urbañczyk-Lipkowska, M. Zia-Ebrahimi and T. W. Panunto, *J. Am. Chem. Soc.* **112**, 8415–8426 (1990); (c) M. C. Etter and S. M. Reutzel, *J. Am. Chem. Soc.* **113**, 2586–2598 (1991); (d) J. Hulliger, *Angew. Chem., Int. Ed. Engl.* **33**, 143–162 (1994); (e) K. Kobayashi, K. Endo. Y. Aoyama and H. Masuda, *Tetrahedron. Lett.* **34**, 7929–7932 (1993); (f) Y. Aoyama, Y. Imai, K. Endo and K. Kobayashi, *Tetrahedron* **51**, 343–352 (1995); (g) G. R. Desiraju, *Angew. Chem., Int. Ed. Engl.* **34**, 2328–2361 (1995).
5. (a) J. A. Zerkowski, C. T. Seto, D. A. Wierda and G. M. Whitesides, *J. Am. Chem. Soc.* **112**, 9025–9026 (1990); (b) J. A. Zerkowski, J. C. MacDonald, C. T. Seto, D. A. Wierda and G. M. Whitesides, *J. Am. Chem. Soc.* **116**, 2382–2391 (1994); (c) J. P. Mathias, E. E. Simanek and G. M. Whitesides, *J. Am. Chem. Soc.* **116**, 4326–4340 (1994).
6. (a) J. M. Lehn, *Angew. Chem., Int. Ed. Engl.* **27**, 89–112 (1988); (b) D. J. Cram, *Angew. Chem., Int. Ed. Engl.* **27**, 1009–1020 (1988); (c) C. J. Pedersen, *Angew. Chem., Int. Ed. Engl.* **27**, 1021–1027 (1988); (d) J. Rebek, Jr, *Angew. Chem., Int. Ed. Engl.* **29**, 245–255 (1990); (e) H. J. Schneider, *Angew. Chem., Int. Ed. Engl.* **30**, 1417–1434 (1991); (f) D. B. Smithrud and F. Diederich, *J. Am. Chem. Soc.* **112**, 339–343 (1990); (g) B. R. Peterson, P. Wallimann, D. R. Carcanague and F. Diederich, *Tetrahedron* **51**, 401–421 (1995); (h) B. J. Whitlock and H. W. Whitlock, *J. Am. Chem. Soc.* **116**, 2301–2311 (1994); (i) J. E. Forman, R. E. Barrans, Jr, and D. A. Dougherty, *J. Am. Chem. Soc.* **117**, 9213–9228 (1995); (j) K. Akari, H. Shimizu and S. Shinkai, *Chem. Lett.*, 295–308 (1993); (k) C. Seel and F. Vötgle, *Angew. Chem., Int. Ed. Engl.* **31**, 528–549 (1992); (l) R. Meric, J.-M. Lehn and J.-P. Visneron, *J. Chem. Soc., Chem. Commun*., 129–131 (1993).
7. (a) H. Ringsdorf, B. Schlarb and J. Venzmer, *Angew. Chem., Int. Ed. Engl.* **27**, 113–158 (1988); (b) M. Ahlers, W. Muller, A. Reichert, H. Ringsdorf and J. Venzer, *Angew. Chem., Int. Ed.*

Engl. **29**, 1269–1285 (1990); (c) K. Fujita, S. Kimura, Y. Imanishi, E. Rump and H. Ringsdorf, *J. Am. Chem. Soc.* **116**, 2185–2186 (1994); (d) D. Lupo, H. Ringsdorf, A. Schuster and M. Seitz, *J. Am. Chem. Soc.* **116**, 10498–10506 (1994).

8. (a) R. S. Mulliken, *J. Am. Chem. Soc.* **74**, 811–825 (1952); (b) M. J. S. Dewar, *J. Am. Chem. Soc.* **83**, 4560–4563 (1961); (c) R. S. Mulliken and W. B. Parson, *Annu. Rev. Phys. Chem.* **8**, 107–126 (1962); (d) R. Foster, *Organic Charge-Transfer Complexes.* Academic Press, New York (1969); (e) R. Foster, *J. Phys. Chem.* **84**, 2135–2141 (1980); (f) C. A. Hunter and J. K. M. Sanders, *J. Am. Chem. Soc.* **112**, 5525–5534 (1990); (g) C. A. Hunter, *Angew. Chem., Int. Ed. Engl.* **32**, 1584–1586 (1993); (h) C. A. Hunter, *J. Mol. Biol.* **230**, 1025–1054 (1993); (i) C. A. Hunter, *Chem. Soc. Rev.* 101–109 (1994); (j) D. Philp, V. Gramlich, P. Seiler and F. Diederich, *J. Chem. Soc., Perkin Trans. 2* 875–886 (1995); (k) F. Cozzi, F. Ponzini, R. Annunziata, M. Cinquini and J. S. Siegel, *Angew. Chem., Int. Ed. Engl.* **34**, 1019–1020 (1995); R. A. Kumpf and D. A. Dougherty, *Science* **261**, 1708–1710 (1993).
9. (a) R. O. Gould, A. M. Gray, P. Taylor and D. Walkinshaw, *J. Am. Chem. Soc.* **107**, 5921–5927 (1985); (b) S. K. Burley and G. A. Petsko, *J. Am. Chem. Soc.* **108**, 7995–8001 (1986); (c) M. Nishio and M. Hirota, *Tetrahedron* **45**, 7201–7245 (1989); (d) M. Nishio, Y. Umezawa, M. Hirota and Y. Takeuchi, *Tetrahedron* **51**, 8665–8701 (1995).
10. (a) B. L. Allwood, H. Shahriari-Zavareh, J. F. Stoddart and D. J. Williams, *J. Chem. Soc., Chem. Commun.*, 1058–1061 (1987), and following papers; (b) J.-Y. Ortholand, A. M. Z. Slawin, N. Spencer, J. F. Stoddart and D. J. Williams, *Angew. Chem., Int. Ed. Engl.* **28**, 1394–1396 (1989); (c) M. Asakawa, P. R. Ashton, S. E. Boyd, C. L. Brown, R. E. Gillard, O. Kocian, F. M. Raymo, J. F. Stoddart, M. S. Tolley, A J. P. White and D. J. Williams, *J. Org. Chem.* **62**, 26–37 (1997).
11. Assuming normal trigonal and tetragonal geometries: [C · · · O]=3.33 Å, [H · · · O]=2.51 Å, C—H · · · O=132° between the central oxygen of the polyether chain of the macrocycle and the methyl group in paraquat. For publications on [CH · · · O] hydrogen bonds, see (a) R. Taylor and O. Kennard, *J. Am. Chem. Soc.* **104**, 5063 (1982); (b) G. R. Desiraju, *Acc. Chem. Res.* **24** 290–296 (1991); (c) V. R. Pedireddi and G. R. Desiraju, *J. Chem. Soc., Chem. Commun.* 988–990 (1992); (d) T. Steiner, *J. Chem. Soc., Chem. Commun.* 2341–2342 (1994).
12. (a) B. Odell, M. V. Reddington, A. M. Z. Slawin, N. Spencer, J. F. Stoddart and D. J. Williams, *Angew. Chem., Int. Ed. Engl.* **27**, 1547–1550 (1988); (b) C. L. Brown, D. Philp and J. F. Stoddart, *Synlett*, 462–464 (1991).
13. (a) P. L. Anelli, P. R. Ashton, R. Ballardini, V. Balzani, M. Delgado, M. T. Gandolfi, T. T. Goodnow, A. E. Kaifer, D. Philp, M. Pietraszkiewicz, L. Prodi, M. V. Reddington, A. M. Z. Slawin, N. Spencer, J. F. Stoddart, C. Vicent and D. J. Williams, *J. Am. Chem. Soc.* **114**, 193–218 (1992); (b) M. Asakawa, P. R. Ashton, S. Menzer, F. M. Raymo, J. F. Stoddart, A. J. P. White and D. J. Williams, *Chem. Eur. J.* **2** 877–893 (1996); (c) T. T. Goodnow, M. V. Reddington, J. F. Stoddart and A. E. Kaifer, *J. Am. Chem. Soc.* **113**, 4335–4337 (1991); (d) A. R. Bernardo, J. F. Stoddart and A. E. Kaifer, *J. Am. Chem. Soc.* **114**, 10624–10631 (1992); (e) S. A. Staley and B. D. Smith, *Tetrahedron Lett.* **37**, 283–286 (1996); (f) R. Castro, K. R. Nixon, J. D. Evanseck and A. E. Kaifer, *J. Org. Chem.* **61**, 7298–7303 (1996).
14. (a) P. R. Ashton, T. T. Goodnow, A. E. Kaifer, M. V. Reddington, A. M. Z. Slawin, N. Spencer, J. F. Stoddart, C. Vicent and D. J. Williams, *Angew. Chem., Int. Ed. Engl.* **28**, 1396–1399 (1989); (b) C. L. Brown, D. Philp, N. Spencer and J. F. Stoddart, *Isr. J. Chem.* **32**, 61–67 (1992).
15. (a) D. B. Amabilino, P. R. Ashton, C. L. Brown, E. Córdova, L. A. Godínez, T. T., Goodnow, A. E. Kaifer, S. P. Newton, M. Pietraszkiewicz, D. Philp, F. M. Raymo, A. S. Reder, M. T. Rutland, A. M. Z. Slawin, N. Spencer, J. F. Stoddart and D. J. Williams, *J. Am. Chem. Soc.* **117**, 1271–1293 (1995); (b) P. R. Ashton, M. A. Blower, S. Iqbal, C. H. McLean, J. F. Stoddart, M. S. Tolley and D. J. Williams, *Synlett* 1059–1062 (1994); (c) P. R. Ashton, M. A. Blower, C. H. McLean, J. F. Stoddart and M. S. Tolley, *Synlett* 1063–1066 (1994).
16. (a) The coalescence methodology was employed to determine values for the rate constant at the coalescence temperature according to I. O. Sutherland, *Annu. Rep. NMR Spectrosc.* **4**, 71–235 (1971); (b) the line-width methodology was employed to determine the kinetic and thermodynamic parameters according to J. Sandström, *Dynamic NMR Spectroscopy.* Academic Press, London (1981).
17. (a) D. B. Amabilino, P. R. Ashton and J. F. Stoddart, *Supramol. Chem.* **5**, 5–8 (1995); (b) D. B. Amabilino, P.-L. Anelli, P. R. Ashton, G. R. Brown, E. Cordóva, L. A. Godínez, W. Hayes, A. E. Kaifer, D. Philp, A. M. Z. Slawin, N. Spencer, J. F. Stoddart, M. S. Tolley and D. J. Williams, *J. Am. Chem. Soc.* **117**, 11142–11170 (1995).
18. P. R. Ashton, M. Blower, D. Philp, N. Spencer, J. F. Stoddart, M. S. Tolley, R. Ballardini, M. Ciano, V. Balzani, M. T. Gandolfi, L. Prodi and C. H. McLean, *New. J. Chem.* **17**, 689–695 (1993).
19. D. B. Amabilino, P. R. Ashton, M. S. Tolley and J. F. Stoddart, *Angew. Chem., Int. Ed. Engl.* **32**, 1297–1300 (1993).
20. P. R. Ashton, J. A. Preece, J. F. Stoddart, M. S. Tolley, A. J. P. White and D. J. Williams, *Synthesis*, 1344–1352 (1994).
21. P. R. Ashton, R. Ballardini, V. Balzani, M. T. Gandolfi, D. J.-F. Marquis, L. Pérez-García, L. Prodi, J. F. Stoddart and M. Venturi, *J. Chem. Soc., Chem. Commun.* 177–180 (1994).
22. P. R. Ashton, R. Ballardini, V. Balzani, A. Credi, M. T. Gandolfi, S. Menzer, L. Pérez-García, L. Prodi, J. F. Stoddart, M. Venturi, A. J. P. White and D. J. Williams, *J. Am. Chem. Soc.* **117**, 11171–11197 (1995).
23. P. R. Ashton, C. L. Brown, E. J. T. Chrystal, T. T. Goodnow, A. E. Kaifer, K. P. Parry, A. M. Z. Slawin, N. Spencer, J. F. Stoddart and D. J. Williams, *Angew. Chem., Int. Ed. Engl.* **30**, 1039–1042 (1991).
24. D. B. Amabilino, P. R. Ashton, A. S. Reder, N. Spencer and J. F. Stoddart, *Angew. Chem., Int. Ed. Engl.* **33**, 1286–1290 (1994).
25. D. B. Amabilino, J. F. Stoddart and D. J. Williams, *Chem. Mater.* **6**, 1159–1167 (1994).
26. M. V. Reddington, N. Spencer and J. F. Stoddart, in *Inclusion Phenomena and Molecular Recognition,* edited by J. L. Atwood, pp. 41–48. Plenum Press, New York (1990).
27. D. Philp, A. M. Z. Slawin, N. Spencer, J. F. Stoddart and D. J. Williams, *J. Chem. Soc., Chem. Commun.* 1584–1586 (1991).
28. M. V. Reddington, A. M. Z. Slawin, N. Spencer, J. F. Stoddart, C. Vicent and D. J. Williams, *J. Chem. Soc., Chem. Commun.* 630–634 (1991).
29. P.-L. Anelli, M. Asakawa, P. R. Ashton, G. R. Brown, W. Hayes, O. Kocian, S. Rodríguez Pastor, J. F. Stoddart, M. S. Tolley, A. J. P. White and D. J. Williams, *J. Chem. Soc., Chem. Commun.* 2541–2545 (1995).
30. P. R. Ashton, C. L. Brown, E. J. T. Chrystal, T. T. Goodnow, A. E. Kaifer, K. P. Parry, D. Philp, A. M. Z. Slawin, N. Spencer,

J. F. Stoddart and D. J. Williams, *J. Chem. Soc., Chem. Commun.* 634–639 (1991).
31. P. R. Ashton, D. Philp, N. Spencer, J. F. Stoddart and D. J. Williams, *J. Chem. Soc., Chem. Commun.* 181–184 (1994).
32. D. B. Ambalino, P. R. Ashton, J. F. Stoddart, S. Menzer and D. J. Williams, *J. Chem. Soc., Chem. Commun.* 2475–2578 (1994).
33. P. R. Ashton, C. G. Claessens, W. Hayes, S. Menzer, J. F. Stoddart, A. J. P. White and D. J. Williams, *Angew. Chem., Int. Ed. Engl.* **34**, 1862–1865 (1995).

